

PACS numbers: 42.55.Px; 42.55.Rz; 61.80.Ba
DOI: 10.1070/QE2007v037n11ABEH013621

Modification of metal film structure by radiation from a diode-pumped solid-state laser for improving the output parameters of high-power laser diodes

V.V. Bezotosnyi, V.Yu. Bondarev, V.I. Kovalenko, O.N. Krokhin, V.F. Pevtsov, Yu.M. Popov, V.N. Tokarev, E.A. Cheshev

***Abstract*. Metal films of heat-removing elements deposited by magnetron sputtering are modified by radiation from a diode-pumped pulsed solid-state Nd : YAG laser to improve the output parameters of high-power laser diodes.**

Keywords: *high-power laser diode, mounting of laser crystals, laser cleaning, modification of metal films.*

1. Relevance of the problem

The technological processes of mounting semiconductor crystals in heat-removing elements of a housing is one of the most important stages in the complete technological cycle of preparation, testing, and certification of ready-made devices because these operations should provide the reliability and a long service life of laser crystals under extreme working conditions. The high quality and long-term stability of the transition between a laser crystal and a heat-removing element providing uniform electric and thermal contacts are key factors facilitating a reliable and long service life of high-power laser diodes.

2. Choice of the metallisation technique

The high-quality metal films of semiconductor crystals and heat-removing elements can be obtained by vacuum sputtering technique. Pure indium films obtained by magnetron sputtering were used as a solder for mounting laser crystals.

The choice of the method is dictated by the following considerations. The thickness of the solder films should be between 2 and 10 μm to obtain a set of the required parameters of the soldered transition used for mounting laser diode crystals or laser diode array crystals. The magnetron sputtering technique is highly efficient and provides the high and stable film deposition rate (in our case, ~ 0.2 μm min^{-1}). Therefore, the film thickness can be simply and precisely controlled during the entire process. The output mirror of the laser diode is the most loaded element of the entire laser crystal because the highest elastic stresses and the maximum temperature and optical power density are concentrated in this region. The conditions of heat removal from the output mirror of the laser crystal are most stringent in this case because the heat flow in this region is close to a one-dimensional flow (in contrast to the two-dimensional flow inside the crystal) [1 – 4]. By using this method, a high degree of adhesion of metal films and a higher-quality deposition of films on the edges of heat-removing elements can be achieved as compared to thermal evaporation. This is very important for carrying out metallisation for mounting traditional laser diodes emitting from the end face.

V.V. Bezotosnyi, V.Yu. Bondarev, V.I. Kovalenko, O.N. Krokhin, V.F. Pevtsov, Yu.M. Popov, E.A. Cheshev P.N. Lebedev Physics Institute, Russian Academy of Sciences, Leninsky prosp. 53, 119991 Moscow, Russia; e-mail: viktorbe@sci.lebedev.ru;
V.N. Tokarev A.M. Prokhorov General Physics Institute, Russian Academy of Sciences, ul. Vavilova 38, 119991 Moscow, Russia

Received 26 April 2007
Kvantovaya Elektronika **37** (11) 1055 – 1059 (2007)
Translated by Ram Wadhwa

3. Properties of magnetron films

We studied the microscopic structure of indium films serving as a solder in mounting high-power laser crystals. Indium is a traditional and most widely used solder material, which is employed for mounting laser crystals due to a number of its attractive properties. These include a low melting point (156 – 161 °C according to different data), high plasticity, availability, and a relatively low cost. The plasticity of indium makes it possible to attain high output parameters of high-power laser diodes in mounting crystals on heat-removing elements made of copper, which is a cheap and available material with a high thermal conductivity (~ 401 W m^{-1} K^{-1} at 300 K [5]), but a rather high (16.7×10^{-6} K^{-1} at 300 K) thermal expansion coefficient (TEC), which differs substantially from the TEC of the semiconductor material of the laser crystal ($\sim 5.8 \times 10^{-6}$ K^{-1} [5]).

We obtained and studied films of thickness varying from 800 Å to 4 μm. Figure 1 shows microphotographs of an indium solder film deposited on the working surface of the heat-removing element. The microphotographs were obtained in a scanning electron microscope with magnifications of 140$^{\times}$ and 4300$^{\times}$. With magnification 140$^{\times}$, the film surface was lusterless, and the microscopic structure in the form of columns (whiskers) and voids could be seen under a magnification of 4300$^{\times}$. The whiskers have a sharp faceting, indicating their crystal structure.

Figure 2 shows the microphotographs of an indium-coated edge of the heat-removing element. One can see that the whisker-type microstructure of the film (see Fig. 1b) is typical of the entire film thickness, and the film covers uniformly the entire edge and partly the lateral face.

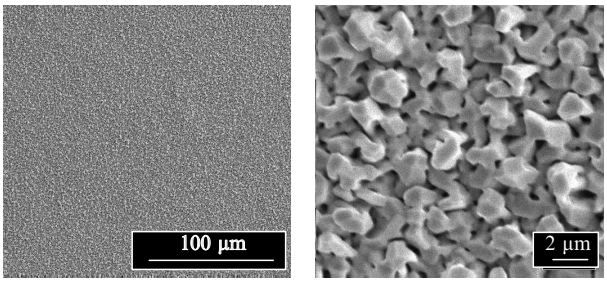

Figure 1. Structure of a 2.7-μm thick indium film observed through a scanning electron microscope under a magnification (a) 140×, and (b) 4300×.

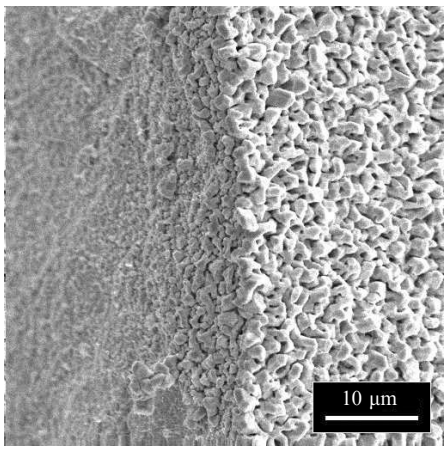

Figure 2. Microphotograph of the structure of an indium film near the working edge of a heat-removing element observed through a scanning electron microscope under a magnification of 1700×.

Structures of films obtained at various temperatures of the substrate and by varying other parameters of the sputtering process (the sputtering rate, the distance between the substrate and the target, etc.) were studied. Shiny films with a highly planar surface could be prepared under certain conditions; however, we have failed to obtain the 'mirror' surface of the film. Apparently, the formation of 'microstructures' in the form of crystallites on the surface and in the bulk of thick films (of indium in our case) obtained by magnetron sputtering is the key problem in high-speed sputtering and is typical of the growth mechanism for films of the vapour–crystal type [6].

4. Experiments on mounting, bulk fusion and solidification of indium films

Experiments on mounting of laser crystals and bulk fusion were performed on the Lambda A6 (Finetech) setup under conditions of a clean local zone of class 100. The melting and solidification of the films was controlled visually and on a screen with the help of a TV camera and a microscope. These processes occurred in pure (99.998 %) nitrogen with a flow rate of 6 L min^{-1}. Heating and cooling rates of up to ~ 20 °C s^{-1} were achieved by using an infrared heater and forced cooling of the working zone. The thermal cycles of the processes were programmed and monitored on computer and video camera screens. The instants of melting and solidification were recorded as tags on the graphic diagram of the process. Various methods of surface preparation, including different etching regimes before sputtering, were used to study the melting of the solder deposited on the copper heat-removing elements. The composition and parameters of metallisation films and the sputtering parameters were varied. This led to the development of metallisation technologies providing reproducible fusion and solidification of the solder without formation of drops and inhomogeneities.

5. Calculation of laser parameters for solder film modification

To improve the efficiency and uniformity of heat removal from a laser crystal, the grain boundaries in the solder film must be destroyed (see Fig. 1b) and remelted for obtaining a homogeneous film. The heating of metals by nanosecond laser pulses provides the conditions of the so-called surface thermal source: $\sqrt{\chi\tau} > \gamma^{-1}$. Here γ is the absorption coefficient of the material (in cm^{-1}), χ is the thermal diffusivity (in $cm^2\ s^{-1}$), and τ is the laser pulse duration. It is also assumed that the heat flow (inside the material) is one-dimensional, which is valid when the inequality $\sqrt{\chi\tau} \ll r$ is satisfied, where r is radius of the radiation spot. This condition is fulfilled for nanosecond pulses when the laser spot radius exceeds 15 μm. It is assumed that the laser pulse is rectangular. Such an idealised pulse shape is convenient for obtaining analytic estimates.

Under these assumptions, the depth h_0 of the melt achieved during a pulse is given by the expression [7–11]

$$h_0(F) = 2(\chi\tau)^{1/2} H_0(F/F_m), \tag{1}$$

where

$$H_0(F/F_m) = \frac{\pi^{1/2}}{1.4}\left\{\left[\frac{2.8}{\pi}\ln\left(\frac{F}{F_m}\right)+1\right]^{1/2} - 1\right\}; \tag{2}$$

$F = I\tau$ is the energy density in a pulse (in J cm^{-2}); I is the pulse intensity (W cm^{-2}), and

$$F_m = \frac{(\pi\chi\tau)^{1/2}}{2A}\rho[C(T_m - T_i) + L_m] \tag{3}$$

is the melting threshold of the material. The surface evaporation effects are not taken into account in expression (1). Thus, the depth h_0 of the melt changes upon variations in the pulse intensity from zero at $F = F_m$ to the maximum value (in the absence of evaporation) $h_{0\max}$ for $F = F_{\max} = F_v$:

$$h_{0\max} = 2(\chi\tau)^{1/2} H_0(F_v/F_m), \tag{4}$$

where

$$F_v = \frac{(\pi\chi\tau)^{1/2}}{2A}\rho[C(T_b - T_i) + L_m] \tag{5}$$

is the evaporation threshold (for this parameter, we conditionally take the pulse energy density at which the normal boiling point T_b is achieved at the surface at the pulse end ($t = \tau$); ρ is the density; C is the specific heat (J g^{-1} deg^{-1}); T_i is the initial temperature; L_m is the latent

heat of melting (J g^{-1}); $A = 4n/[(n+1)^2 + k^2]^{-1}$ is the absorptivity of the material; n and k are the real and imaginary parts of the refractive index at a wavelength of 1.06 μm; and $\gamma = 4\pi k/\lambda$ is the above-mentioned absorption coefficient of the material (cm^{-1}).

After termination of the pulse ($t > \tau$), the melt thickness continues to increase from $h(t = \tau) = h_0$ to the maximum value $h = h_1$ for $t = t_{max}$ due to an excess enthalpy stored in the melt layer during the pulse. Solidification begins for $t > t_{max}$: the melt layer thickness decreases from for $h = h_1$ to zero for $t = t_s$, where t_s is the instant of complete solidification. Lower (h_{11}) and upper (h_{12}) bounds for h_1 (i.e., $h_{11} < h < h_{12}$) are given by the expression [7–11]

$$h_{11}(F/F_m) = \frac{(\pi\chi\tau)^{1/2}}{2}\left[\frac{F}{F_m} - \frac{1}{1 + 0.4953H_0(F/F_m)}\right], \quad (6)$$

$$h_{12}(F/F_m) = 2(\chi\tau)^{1/2}\frac{1}{0.246} \times \left[1 - \left(1 - 2 \times 0.246 \ln\frac{F}{F_m}\right)^{1/2}\right] \text{ for } F/F_m < 6.7, \quad (7)$$

$$h_{12}(F/F_m) = \frac{(\pi\chi\tau)^{1/2}}{2}\frac{F}{F_m} = \frac{AF}{\rho[C(T_m - T_i) + L_m]} \text{ for } F/F_m \geqslant 6.7. \quad (8)$$

For indium, we have $\rho = 7.3$ g cm^{-3}, $C(0-150\,^{\circ}C) = 0.234$ J g^{-1} K^{-1}, $T_i = 20\,^{\circ}C$, $T_m = 157\,^{\circ}C$, $T_b = 2024\,^{\circ}C$, $L_m = 28.4$ J g^{-1} [3], and $\chi = 0.4$ cm^2 s^{-1}. In our case, the actual values of n and k at $\lambda = 1.06$ μm are determined by the structural properties of the surface. Moreover, these quantities are dynamic parameters during laser processing (i.e. vary upon a change in the film microstructure). The values of the coefficient A are estimated as 0.1–1. For a pulse duration $\tau = 6$ ns, we obtain from these expressions:

For $A = 0.1$: $F_m = 0.19$ J cm^{-2}, $F_v = 1.5$ J cm^{-2}. For $F = F_v$, we have $h_0 = 0.87$ μm, $h_{11} = 3.4$ μm, and $h_{12} = 3.6$ μm.

For $A = 0.2$: $F_m = 0.09$ J cm^{-2}, $F_v = 0.79$ J cm^{-2}. For $F = F_v$, we have $h_0 = 0.87$ μm, $h_{11} = 3.3$ μm, and $h_{12} = 3.6$ μm (i.e. $h_1 = 3.5$ μm).

For $A = 0.5$: $F_m = 0.038$ J cm^{-2}, $F_v = 0.32$ J cm^{-2}. For $F = F_v = 0.32$ J cm^{-2}, we have $h_0 = 0.87$ μm, $h_{11} = 3.4$ μm, and $h_{12} = 3.6$ μm (i.e. $h_1 \simeq 3.5$ μm). For $F = 0.24$ J cm^{-2}, we have $h_1 \simeq 2.7$ μm.

For $A = 1$: $F_m = 0.019$ J cm^{-2}, $F_v = 0.16$ J cm^{-2}. For $F = F_v = 0.16$ J cm^{-2}, we have $h_0 = 0.87$ μm, $h_{11} = 3.4$ μm, and $h_{12} = 3.6$ μm (i.e. $h_1 \simeq 3.5$ μm). For $F = 0.12$ J cm^{-2}, we have $h_1 \simeq 2.7$ μm.

These estimates of the required laser pulse energy density and the melt thickness were used for determining the laser parameters required for processing In films. The maximum output energy of the laser exceeded 100 μJ and the maximum pulse energy density exceeded 0.32 J cm^{-2} for a spot diameter ~ 200 μm at the $1/e^2$ level. A laser diode was used as the pump source. According to our estimates, this energy density for a beam diameter of ~ 200 μm exceeds the melting threshold for $A = 0.1 - 1$ and the evaporation threshold for $A > 0.5$. For $A = 0.1$, the evaporation threshold can be achieved for a tighter focusing of the beam into a spot of diameter ~ 90 μm.

6. Experiment on laser-induced modification of metal films

Upon bulk heating of a substrate together with the solder film, the coalescence of whiskers is prevented by the developed surface of grain boundaries, oxidation and contamination of this surface in air, as well as by the inhomogeneities of the film structure and meniscus. As mentioned above, experiments on modification of solder films were performed by using a specially developed diode-pumped pulsed solid-state laser, which was Q-switched with the help of an intracavity acousto-optical modulator. Figure 3 shows the scheme of this laser. The threshold current of the semiconductor pump laser was 0.7 A, the slope of the light–current characteristic was 1.15 W A^{-1}, and the maximum cw power was ~ 5 W. The pulsed solid-state laser had the following parameters:

Radiation wavelength/μm	1.064
Mode composition	TEM_{00}
Beam diameter/mm	0.22 at $1/e^2$ level
Beam divergence/mrad	6.5
Polarisation	linear (more than 100:1)
Pulse repetition rate/kHz	to 300
Pulse duration/ns	6–140
Stability (% h^{-1})	1
Emitting head size/mm	35 × 55 × 140
Weight/kg	0.8

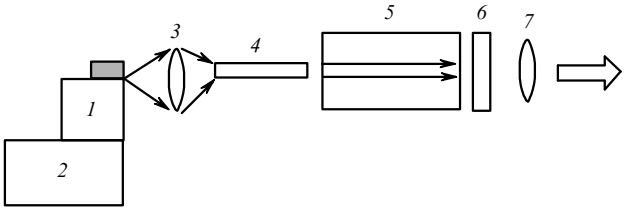

Figure 3. Scheme of a diode-pumped solid-state laser: (*1*) semiconductor pump laser assembled on a heat-removing element of the C-mount type; (*2*) thermoelectric cooler; (*3*) focusing optics; (*4*) Nd : YAG crystal; (*5*) acousto-optic modulator; (*6*) output mirror; (*7*) collimator.

The output power of the solid-state laser was varied by regulating the pump current in the semiconductor laser in accordance with Table 1.

For laser-beam scanning, the heat-removing element being processed was fixed on a computer-controlled xy optical stage. The scan step and the laser pulse energy were varied for determining the optimal processing regimes. The maximum pulse power of the solid-state laser was ~ 15 kW

Table 1. Dependence of the average power of a pulsed solid-state laser at a pulse repetition rate of 5 kHz on the pump current from a cw laser diode.

Pump current/A	Average power/W
1.04	0
1.25	0.012
1.5	0.054
2.04	0.142
2.5	0.22
3.05	0.33
3.47	0.426
3.8	0.5

for a pulse duration of 6.5 ns and a pulse repetition rate of 5 kHz. Accordingly, the maximum pulse energy was ~ 100 μJ.

7. Discussion of results

Figure 4 shows the microstructure of the film in the laser radiation region and outside it. Optical and scanning electron microscopy revealed an improvement in the microscopic structure of the film after irradiation for a total beam energy of ~ 3 μJ and a beam diameter of 160 μm at the $1/e^2$ level. The experimentally determined diameter of the whisker coalescence region was ~ 35 μm for the case when the film was molten over the entire depth. If melting did not occur over the entire depth of the film, the transition region was ~ 5 μm. The total energy incident in this region was ~ 1 μJ, and the mean density of the incident radiation energy was ~ 0.1 J cm^{-2}. A hot plume was observed and a shock-wave noise was heard when the above energy density was achieved and at higher irradiation levels.

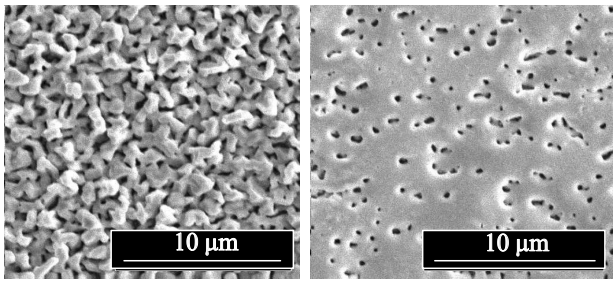

Figure 4. Structure of a 2.7-μm thick indium film (a) before and (b) after laser processing, observed through a scanning electron microscope under a magnification of 4300×.

This value of the energy density is between the values corresponding to the theoretical estimate of melting and evaporation thresholds for $A = 0.5$. According to the observations made through a microscope, the thickness of the modified film was 2.5 times smaller than the thickness of the initial porous film. Taking this fact into account, we found that the experimental estimates of the energy density (~ 0.1 J cm^{-2}) of the modified film thickness (~ 1 μm) are in good agreement with the theoretical values of the parameters for $A = 0.5$ and $F = 0.1$ J cm^{-2}, which are found to be $h_0 = 0.45$ μm, $h_{11} = 0.79$ μm, and $h_{12} = 1.1$ μm. The melt depth, estimated approximately as $h_1 = \frac{1}{2}(h_{11} + h_{12})$, was found to be 0.95 μm. Note that the value $A = 0.1$ is typical for smooth surface of a metal film [12] while its value for a surface with micropores (like the one in our case) is probably 0.3–05, depending on the shape and size of the pores and the volume occupied by them. For a radiation energy density of ~ 0.3 J cm^{-2}, the indium film evaporates in the maximum energy density region of the laser spot; the diameter of the evaporation zone is ~ 10 μm. As the energy density is increased, the diameter of the evaporation zone of indium increases and the material of the heat-removing element begins to evaporate at the centre of the spot.

Laser processing improved the homogeneity of the surface and the film structure (see Fig. 4b). After laser processing, the film acquires features of an amorphous structure probably due to rapid (nanosecond) melting and cooling of the material in the irradiated region.

Thermal expansion of indium (especially after transition through the melting point) during heating from room temperature to the evaporation temperature may produce a strong mechanical damage of the oxide film at grain boundaries, which is important for grain coalescence and for obtaining a more continuous and homogeneous coating.

After the laser-induced modification of the indium layer, the efficiency of heat removal from the semiconductor laser crystal may substantially increase because the area on which the solder interacts with the metal film on the laser crystal after bulk melting increases; the thermal conductivity of the solder layer also increases due to the decrease in the number of pores. Consequently, when such modified films are used, one can expect considerable improvement of the output parameters of high-power semiconductor devices (especially high-power laser diodes). Note that the microscopic structure of the initial and treated films (see microphotographs) is far from perfect and defects are observed at the surface and in the bulk after laser processing. These defects generally have a rounded shape and a diameter from 0.1 to 1 μm. To reduce the number of defects and obtain a more homogeneous structure of the surface, we plan to improve the laser processing technique.

The above assumption concerning the possibility of improvement of heat removal from semiconductor crystal by using laser-processed metal films were verified in mounting the crystals of high-power diode lasers on solder films subjected to laser processing and without it. Figure 5 shows typical light–current characteristics for two lasers operating at a wavelength of 808 nm. We used heat-removing elements from the same batch, which were metallised in a single evaporation process. Laser crystals were also chosen from the same batch. The threshold currents of the lasers differed insignificantly. For a current of 4.3 A, the power of LD laser No. 1 assembled upon laser modification of the indium film was 4 W. The maximum of the envelope of the laser emission spectrum (at $T = 25\,^{\circ}$C) was observed at 808.3 nm, the half-width of the spectrum was 1 nm, and the temperature coefficient of wavelength shift was 0.23 nm K^{-1}, which satisfies the requirements imposed on the pump sources for Nd : YAG crystals. From the

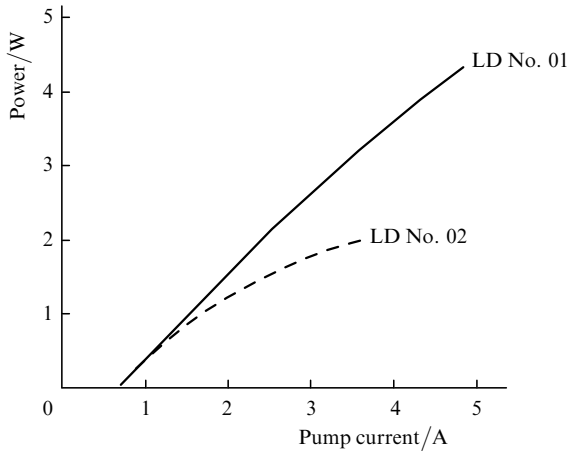

Figure 5. Light–current characteristics of high-power cw diode lasers at a temperature of 25 °C; LD No. 1 (with laser processing of the metal film) and LD No. 2 (without laser processing).

technological point of view, such spectral parameters indicate a high uniformity of heat removal from the crystal. Short-term tests of the diodes assembled by using laser processing showed that their output power (4 W) did not change after 100 h of their operation to within the error of measurements. The maximal power of LD No. 01 laser was 5 W for a current of 6 A. The maximum of the radiation spectrum envelope for LD laser No. 02 was red-shifted relative to that for LD No. 01 due to insufficiently efficient and nonuniform heat removal. The half-width of its emission spectrum was 2 nm for a pump current of 3 A. The maximum power of LD No. 02 laser assembled without laser modification of the indium film was only 2 W, while power saturation was observed for a current of 4.5 A.

8. Conclusions

It has been shown that laser processing modifies the microscopic structure of metal films, in particular, reduces the porosity and roughness of the surface, destroys oxide films, and cleans the surface from contamination. The estimates of the energy density and depth of remelted indium layer obtained on the basis of the computational model for surface absorbability $A = 0.5$ are in good agreement with the estimates obtained on the basis of experimental results. These properties of the modified surface make it possible to reproducibly obtain high radiative parameters in mounting high-power laser diodes operating at a wavelength of 808 nm, which meet the requirements imposed of the pump sources for Nd : YAG crystals.

The technique developed here for modifying the structure of metal films can be used in various micro- and optoelectronic technologies.

Acknowledgements. The authors thank I.V. Akimova who carried out scanning electron microscope studies. This work was supported the Russian Foundation for Basic Research (Grant Nos 05-08-65399 and 06-02-08058-ofi) and by a grant from the President of Russian Federation under a state program supporting leading science schools (Grant No. NSh-6055-2006.2).

References

1. Bezotosnyi V.V., Kumykov Kh.Kh., Markova N.V. *Kvantovaya Elektron.*, **23**, 775 (1996) [*Quantum Electron.*, **26**, 755 (1996)].
2. Bezotosnyi V.V., Kumykov Kh.Kh., Markova N.V. *Kvantovaya Elektron.*, **24**, 495 (1997) [*Quantum Electron.*, **27**, 481 (1997)].
3. Bezotosnyi V.V., Kumykov Kh.Kh. *Kvantovaya Elektron.*, **25**, 225 (1998) [*Quantum Electron.*, **28**, 217 (1998)].
4. Basov N.G., Bezotosny V.V., Kumykov Kh.Kh., Popov Yu.M. *Laser and Particle Beams* (USA, Cambridge: Cambridge University Press, 1999) Vol. 17, No. 3, pp 427–436.
5. *Fizicheskie velichiny, Spravochnik* (Handbook of Physical Quantities) (Moscow: Energoatomizdat, 1991).
6. Palatnik L.S., Fuks M.Ya., Kosevich V.M. *Mekhanizm obrazovaniya i substruktura kondensirovannykh plenok* (Mechanism of Formation and Substructure of Condensed Films) (Moscow: Nauka, 1977).
7. Tokarev V.N., Kaplan A.F.H. *Lasers in Engineering,* **7** (3–4), 295 (1998).
8. Tokarev V.N., Kaplan A.F.H. *J. Appl. Phys.*, **86**, 2836 (1999).
9. Tokarev V.N., Kaplan A.F.H. *J. Phys. D: Appl. Phys.*, **32**, 1526 (1999).
10. Lazare S., Tokarev V.N., in *Recent Advances in Laser Processing of Materials*. Ed. by J. Perriere, E. Millon, E. Fogarassy (Amsterdam: Elsevier, 2006) Ch. 5.
11. Tokarev V.N. *Laser Phys.*, **16** (9), 1291 (2006).
12. Delone N.B. *Vzaimodeistvie lazernogo izlucheniya s veshchestvom* (Interaction of Laser Radiation with Matter) (Moscow: Nauka, 1989).